Concerted and Stepwise Mechanisms in Metal-Free and Metal-Assisted [4+3] Cycloadditions Involving Allyl Cations

Israel Fernández,*[a] Fernando P. Cossío,*[b] Abel de Cózar,[b] Agustí Lledós,[c] and José Luis Mascareñas[d]

Abstract: The thermal [4+3] cycloaddition reaction between allenes and tethered dienes (1,3-butadiene and furan) assisted by transition metals (Au^I, Au^{III}, Pd^{II}, and Pt^{II}) was studied computationally within the density functional theory framework and compared to the analogous non-organometallic process in terms of activation barriers, synchronicity and aromaticity of the corresponding transition states. It was found that the metal-mediated cycloaddition reaction is concerted and takes place via transition structures that can be even more synchronous and more aromatic than their non-organometallic analogues. However, the processes exhibit slightly to moderately higher activation barriers than the parent cycloaddition involving the hydroxyallylic cation. The bond polarization induced by the metal moiety is clearly related to the interaction of the transition metal with the allylic π* molecular orbital, which constitutes the LUMO of the initial reactant. Finally, replacement of the 1,3-butadiene by furan caused the transformation to occur stepwise in both the non-organometallic and metal-assisted processes.

Keywords: aromaticity · catalysis · cycloadditions · density functional calculations · reaction mechanisms

Introduction

The [4C+3C] annelation of dienes and allyl cation derivatives, constitutes a convenient way to prepare relatively complex seven-membered rings from simple starting materi-
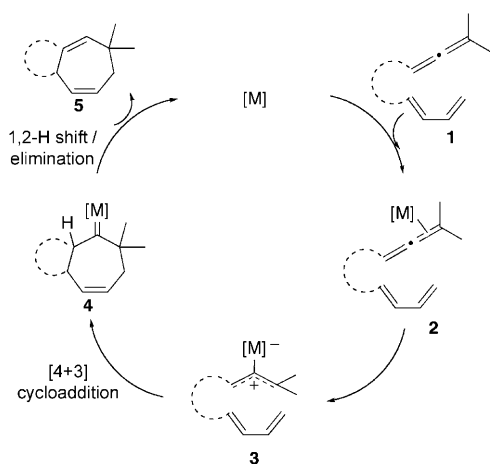
[a] Dr. I. Fernández
Departamento de Química Orgánica, Facultad de Química
Universidad Complutense, 28040 Madrid (Spain)
Fax: (+34) 913944310
E-mail: israel@quim.ucm.es

[b] Prof. Dr. F. P. Cossío, Dr. A. de Cózar
Departamento de Química Orgánica I-Kimika Organikoa I Saila
Facultad de Química-Kimika Fakultatea
Universidad del País Vasco-Euskal Herriko Unibertsitatea
P. K. 1072, 20080 San Sebastián-Donostia (Spain)
Fax: (+34) 9430-15270
E-mail: fp.cossio@ehu.es

[c] Prof. Dr. A. Lledós
Departament de Química, Universitat Autònoma de Barcelona
08193-Bellaterra, Barcelona (Spain)

[d] Prof. Dr. J. L. Mascareñas
Departamento de Química Orgánica
Facultad de Química Universidad de Santiago de Compostela
15782-Santiago de Compostela (Spain)

Supporting information for this article is available on the WWW under http://dx.doi.org/10.1002/chem.201001714; Cartesian coordinates (Å) and total energies (a.u., noncorrected zero-point vibrational energies included) of all the stationary points discussed in the text.

als.[1,2] However, the standard methodologies, which mainly involve oxy- and amino-allyl cations, usually present important limitations, that is, unstable allyl cation precursors or the need for stoichiometric activators,[3] and the requirement of conformationally restricted dienes (furans or cyclopentadienes). To avoid these shortcomings, some of us recently reported a novel metal (Pt and Au)-catalyzed [4C+3C] cycloaddition between dienes and tethered allenes, which provides a short and stereoselective route to synthetically useful bicyclo[5.3.0]decane skeletons like **5**.[4,5] Most probably, the reaction involves a concerted [4+3] cycloaddition from the initially formed complex **3** to produce the metal–carbene complex **4** and subsequent 1,2-H-shift with simultaneous coordination of the newly formed C≡C double bond to the metal (Scheme 1).[5]

Similar to other pericyclic reactions, such as [4+2] Diels–Alder or [3+2] cycloadditions, it is very likely that both metal-free and metal-catalyzed [4+3] transformations occur through highly concerted and aromatic transition states. In fact, the aromaticity of the transition states associated to pericyclic reactions is a well-known issue that has been also studied computationally,[6] usually by using the magnetic nuclear independent chemical shift (NICS) values.[7] In the context of our ongoing interest in metal-mediated cycloadditions, we recently reported that both [3+2][8] and [4+2][9] cycloadditions involving Fischer-type carbene complexes

Scheme 1. Proposed reaction mechanism for the Au^I or Pt^{II}-catalyzed [4+3] annulation.

occur concertedly via transition structures that are more asynchronous and less aromatic than their non-organometallic analogues—a behavior that is extensible to the reactions involving Lewis acid complexed acrylates.

Here, we present a comparison between classical oxyallyl cation-diene cycloadditions and the analogous reaction involving a metal moiety, in terms of activation barriers, synchronicity, and aromaticity of the corresponding transition states. Moreover, the factors that control the concertedness of the process are analyzed theoretically.

Results and Discussion

We first analyzed the parent non-organometallic cycloaddition reaction, which involves the hydroxyallyl cation **3a**. Although similar processes were studied computationally by Cramer and co-workers,[10] no insight into the synchronicity and aromaticity of the process has been reported so far. As readily seen in Scheme 2, the cycloaddition reaction occurs concertedly with a quite low energy barrier due to the high resemblance between the starting reactant **3a** and transition state, **TSa**. Interestingly, the computed synchronicity ($S_y = 0.83$) indicates that the transformation is quite synchronous.
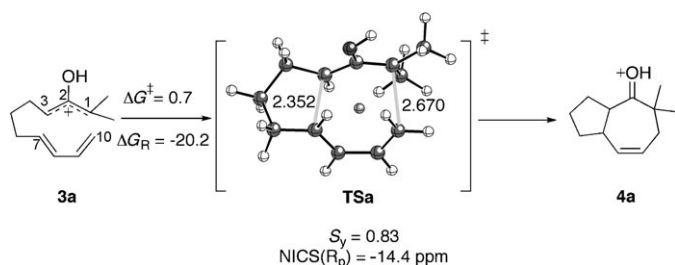
Scheme 2. The [4+3] cycloaddition of cation **3a**. Bond lengths are given in Å and energies (placed close to arrows) in kcal mol^{-1}. The dummy atom in the center of the rings being formed indicates the (3,+1) ring critical point of the electron density of the saddle point **TSa**.

The deviation from the perfect synchronicity might be the result of the different C−C bond orders in the saddle point, that is, the bond development of the C3−C7 is higher (Wiberg NBO bond order of 0.26) than for C1−C10 (NBO bond order of 0.16; see Scheme 2 for the corresponding bond lengths).[11]

We also computed the NICS values at the (3,+1) ring critical point of the electron density to prove the aromaticity of **TSa**. Given the unsymmetrical character of our cyclic systems, we needed to define the inner points unambiguously. The (3,+1) ring critical point of the electron density, as defined by Bader,[12] is an unambiguous choice for the calculation of the NICS values, since only at this point is the electron density a minimum with respect to motion on the ring's plane and maximum with respect to motion perpendicular to the plane defined by the ring. Thus, the calculated highly negative isotropic NICS(R_p) value (−14.4 ppm) confirms the aromatic character of the saddle point.

The expected diamagnetic shielding σ_{zz}^d in the ring formed in **TSa** was computed according to our previously described model:[13b]

$$\sigma_{zz}^d = \frac{e^2 \mu_o}{8\pi m_e} R_{av}^{-1} \left[1 + \left(\frac{z - R_o}{R_{av}} \right)^2 \right]^{-3/2} \quad (1)$$

In this expression, it is assumed that the diatropic ring current is confined into a circumference of radius R_{av} and circulates at a R_o distance above the ring point. The maximum value of σ_{zz}^d, denoted as σ_{max}^d, is achieved when $z = R_o$. For $R_{av} = 1.466$ Å and $R_o = 0.2$ Å, it was found that $\sigma_{max}^d = -9.6$ ppm, which accounts for approximately 67% of the NICS at the ring point. In addition, it was found that the ratio $\sigma_{zz}^d/\sigma_{max}^d$ behaves similarly to NICS/NICS$_{max}$ along the z axis; this confirms that the aromatic character of **TSa** can be interpreted in terms of a diatropic ring current circulating along the ring being formed by the concerted and symmetry-allowed cycloaddition process (Figure 1 A).

Therefore, we can propose that the six electrons involved in the cycloaddition give rise to an appreciable ring current, which in turn, promotes a strong diamagnetic shielding at the ring critical point, leading to the observed NICS values. Although this method has been proved to work nicely in confirming the aromaticity of the so-called *in-plane* aromatic transition states,[8,9,13] it has been repeatedly reported that the isotropic NICS values might lead to misleading results due to local contributions of the σ framework.[14] For this reason, we also applied the anisotropy of the induced current density (AICD) method, developed by Herges and co-workers,[15] to visualize the delocalization of electrons that are responsible for the aromaticity. As showed in Figure 1 B, the delocalization of the electrons can be clearly seen within the seven-membered cyclic array, which produces the diamagnetic current responsible for the computed negative NICS value.

The effect of the metal fragment in the analogue cycloaddition reaction between *meta* stabilized allyl cations and bu-
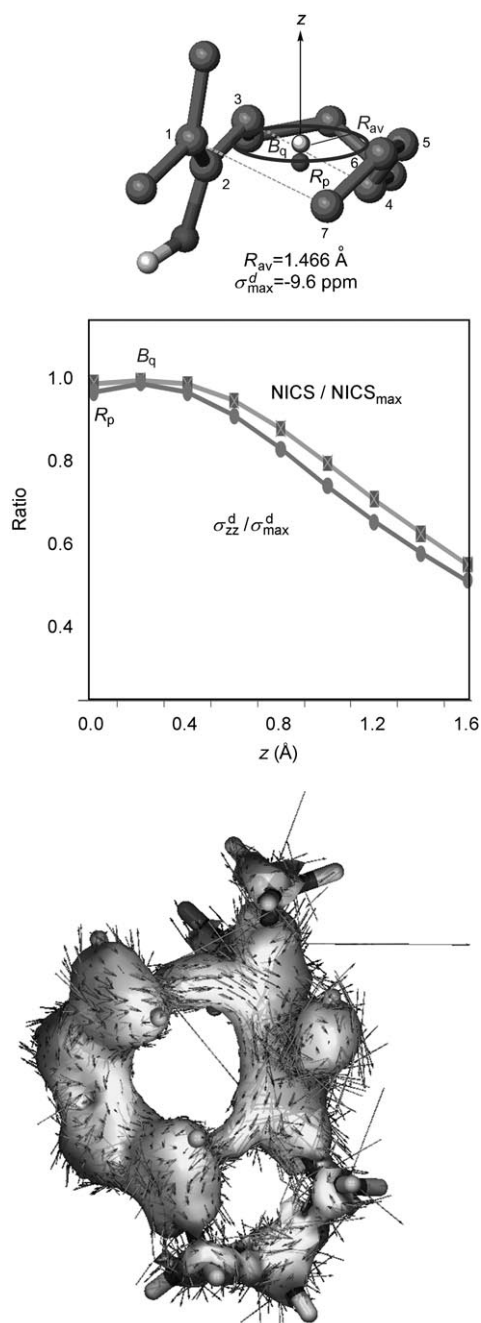
Figure 1. A) Analysis of the aromaticity of transition structure **TS a** according to the ring current model. B) AICD plot of the transition state **TS a** (isosurface value of 0.045).
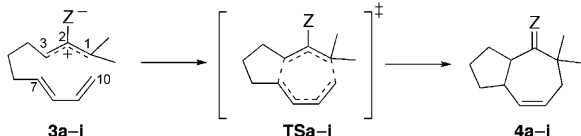
tadiene was studied next. Table 1 shows the most relevant data of these transformations involving Au^{I}, Au^{III}, Pd^{II}, and Pt^{II} complexes. Similar to the process involving compound **3a**, it was found that the metal-assisted cycloadditions are concerted and occur via the transition states depicted in Figure 2. One of the most striking differences between the parent and the metal-mediated cycloadditions was revealed by inspection of the structures of the corresponding transition states. As readily seen in Table 1 and Figure 2, the C1—

C10 bond lengths are always shorter than the C3—C7 distances in **TS b–i** while the contrary is found in **TS a**. Moreover, whereas the C1—C10 bond is clearly emerging in **TS a** (2.670 Å, NBO bond order of 0.16), it is nearly developed in **TS b–i** (2.248–2.378 Å, NBO bond order in the range of 0.28–0.35). This is mainly due to the bond polarization induced by the presence of the metal moiety as indicated by the charge of the C1 and C2 carbon atoms in the reactants **3a–i**. For instance, the computed NBO charge for C1 varies from $+0.09$ a.u. in the parent compound **3a** to $+0.23$ a.u. in **3d** (or $+0.20$ a.u. in the neutral complex **3i**). Strikingly, the NBO charge for C2 is $+0.29$ in **3a** while a negative value of -0.42 a.u. is found in **3d** (-0.16 a.u. in complex **3i**). The close relationship between the bond polarization in the initial reactants **3**, measured by the computed NBO charges on C1 and C2 carbon atoms and the C1—C10 bond lengths of the corresponding transition states, is nicely reflected in the very good linear correlations that were found when both parameters were plotted (C1—C10 bond lengths vs. NBO charge on C1: correlation coefficient of 0.96 and standard deviation of 0.01; C1—C10 bond lengths vs. NBO charge on C2: correlation coefficient of 0.97 and standard deviation of 0.05; Figure 3).

The above-mentioned changes induced by the metal moiety in the geometry of the respective saddle points are also translated into quite significant alterations in terms of the computed barrier heights. For instance, from practically a no-barrier process in the cycloaddition reaction of the parent cation **3a** ($\Delta G^{\neq}_{298} = 0.7$ kcal mol^{-1}; Table 1, entry 1), a value of 12.1 kcal mol^{-1} was found for the transformation involving the Au^{I} cationic complex **3e**, which in any case represents an activation barrier that should be easily surmountable at room temperature. Interestingly, no systematic differences were found between the considered metal chlorides in terms of the computed activation barriers (variation within ca. 2 kcal mol^{-1}; Table 1, entries 2 and 8–10), which suggests that the metal (Au, Pt, or Pd) has little effect in the cycloaddition reaction. Thus, it is not surprising that similar values of activation and reaction energies were found in the series of Au^{I} complexes bearing different σ donor ligands, such as phosphines (Table 1, entries 3–5) or N-heterocyclic carbene (entry 7).

Interestingly, we have found that the characteristics of the LUMO of reactants **3b–i**, which corresponds to the π* molecular orbital of the allylic fragment (Figure 4), are clearly determined by the metal moiety. Thus, by means of the second-order perturbation theory of the NBO method, stabilizing two-electron delocalizations from occupied d atomic orbitals of the metal atom to the π* molecular orbitals of the allylic fragment were found. For instance, for complex **3d**, the computed associated second-order perturbation energies for these delocalizations are -3.2 and -2.6 kcal mol^{-1} for the d→π* (C3—C2) and d→π* (C1—C10) delocalizations, respectively. As the LUMO is involved in the cycloaddition process (vide infra), the effect of the metal fragment in this transformation is in part due to these stabilizing interactions.

Table 1. Computed data for the [4+3] cycloaddition reaction of compounds **3a–i**. All values have been computed at the B3LYP/def-SVP level.

Entry	Z	$\Delta G^{\neq}_{298}$[a]	$\Delta G_{R,298}$[b]	r (C3–C7)[c]	r (C1–C10)[c]	q(C1)[d]	q(C2)[d]	E_{LUMO}[e]	S_y	NICS(R_p)[f]
1	a, OH⁺	0.7	−20.2	2.352	2.670	0.090	0.292	−6.90	0.83	−14.4
2	b, AuCl	4.0	−19.5	2.382	2.331	0.171	−0.410	−3.40	0.86	−17.6
3	c, [AuPH₃]⁺	8.6	−3.9	2.493	2.254	0.225	−0.439	−6.62	0.75	−17.1
4	d, [AuPMe₃]⁺	10.7	−4.3	2.476	2.259	0.230	−0.420	−6.39	0.85	−17.3
5	e, [AuPPh₃]⁺	12.1	−3.6	2.468	2.264	0.227	−0.404	−6.14	0.87	−17.3
6	f, [AuNHC]⁺[g]	10.5	−4.8	2.465	2.265	0.240	−0.430	−6.27	0.85	−17.4
7	g, AuCl₃	6.3	−10.5	2.405	2.292	0.212	−0.328	−4.10	0.78	−17.1
8	h, PdCl₂	5.2	−17.5	2.379	2.364	0.199	−0.160	−3.76	0.83	−17.3
9	i, PtCl₂	4.8	−23.4	2.493	2.378	0.197	−0.160	−3.72	0.83	−16.3

[a] Activation barrier ($\Delta G^{\neq}_{298}$, in kcal mol⁻¹) values computed as $\Delta G^{\neq}_{298} = G(\mathbf{TS}) - G(\mathbf{3})$. [b] Reaction energy ($\Delta G_{R,298}$, in kcal mol⁻¹) values computed as $\Delta G_{R,298} = G(\mathbf{4}) - G(\mathbf{3})$. [c] Bond lengths in the transition state (Å). [d] NBO charges of the carbon atom in the transition state [a.u.]. [e] LUMO energies of reactants **3** [eV]. [f] NICS values [ppm] at the (3,+1) ring critical point of the **TS**. [g] NHC: imidazol-2-ylidene.
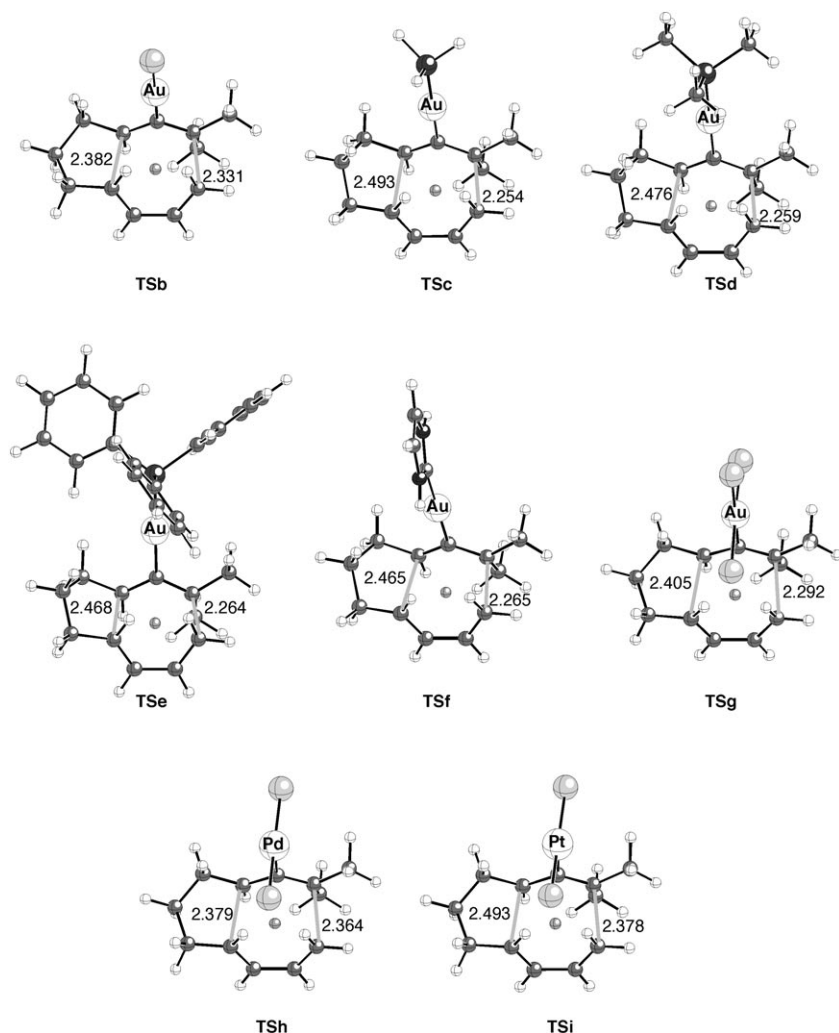

Figure 2. Chief geometric features of transition structures associated with [4+3] cycloaddition reaction of complexes **3b–i**. Bond lengths are given in Å. Chlorine atoms are represented as larger spheres. See Scheme 2 legend for additional details.

In terms of the computed synchronicity, the data in Table 1 clearly show that the concerted metal-assisted cycloadditions exhibit moderate to high synchronicities (S_y values in the range of 0.75–0.87). In fact, a value of about 0.9 can be reached in complexes **3b** or **3e**, thus indicating that the metal-mediated transformations can be even more synchronous than the corresponding parent reaction of the hydroxyallylic cation **3a**. This behavior is clearly different to other metal-assisted cycloadditions like [3+2] or [4+2] processes,[8,9] which occur with lower values of synchronicity with respect to the corresponding non-organometallic reactions. Perhaps this fact is related to the bonding of the metal to the central atom of the allylic moiety, since this carbon atom bears no LUMO coefficient at the parent allyl cation. The effect of the solvent in the cycloaddition process was computed next by using the SCRF approach under the Onsager–Kirkwood formalism[15] with sequential single-point calculations at the gas phase optimized geometries of the parent compound **3a** and complexes **3d** and **3i**. The data compiled
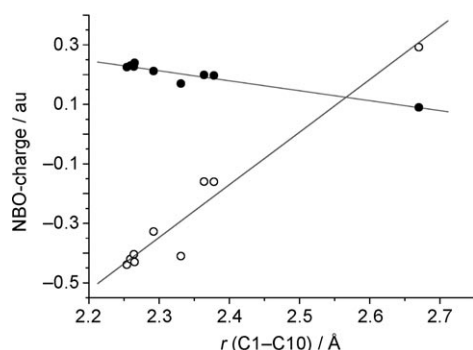
Figure 3. Plot of the (C1−C10) bond lengths in **TS a–i** versus the NBO charges of the C1 (●) and C2 (○) carbon atoms.
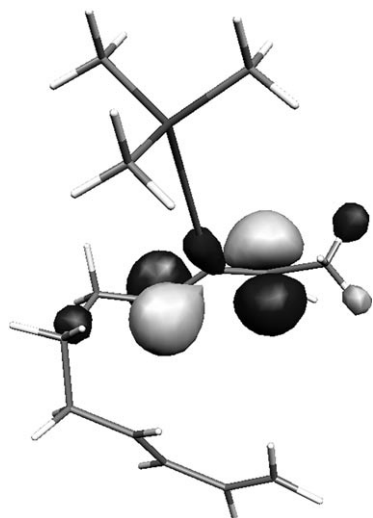

Figure 4. LUMO of complex **3d** (isosurface value of 0.040).

in Table 2 indicate that the activation barriers of the cycloaddition reaction are slightly larger in solution than in the gas phase for the cationic species **3a** and **3d**. This was expected because the large cationic character of the reactants diminishes along the reaction coordinate, thereby resulting in lower solvation energies for the transition structures with respect to the starting products. On the contrary, slightly lower barrier energies were found for the neutral complex **3i**, thus indicating a higher solvation energy in the corresponding saddle point **TS i** than in the initial complex **3i**. From the above data, it can be safely concluded that the effect of the solvent in the cycloaddition reaction is not es-
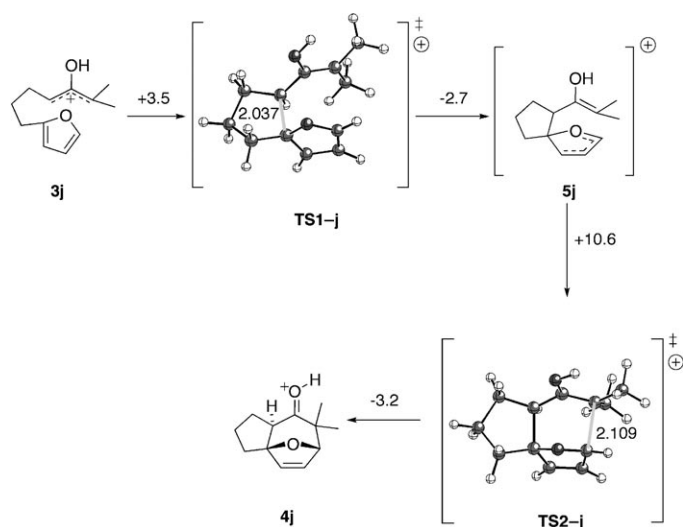
pecially relevant in terms of the computed activation barriers.

The effect of the metal moiety in the aromaticity, which had been already assessed for the analogous non-metallic cycloaddition, was also addressed. Likewise, the magnetic properties of the corresponding transition structures were computed by using the nucleus-independent chemical shifts (NICSs) at the $(3,+1)$ ring critical point of the electron density. The position of the ring critical points of **TS b–i** are indicated in Figure 2 and the NICSs at these points are compiled in Table 1. All transition structures exhibit high negative NICSs values (ranging from -16.3 ppm in **TS i** to -17.6 ppm in **TS b**), which can be attributed to the strong diamagnetic shielding due to the strong aromatic character of these TSs. If we assumed that, in transition states, bonding equalization and synchronicity characterize aromatic structures,[16] it is not surprising that the NICS values obtained for saddle points **TS b–i** are slightly higher than that found for the parent cycloaddition reaction involving **TS a**. This becomes obvious when the bond lengths of the newly forming carbon−carbon bonds (C3−C7 and C1−C10) in the respective TSs are compared. Table 1 and Figure 2 clearly show a higher bond equalization in the saddle points **TS b–i** compared to **TS a**, which is translated to a higher value of aromaticity (measured by the NICS values).

We should point out that no correlation between the NICS values and the activation barriers was found. This result indicates that the gain in stability by aromaticity does not play a major role in controlling the barrier heights of the studied processes. We have reported a similar finding in different double group transfer reactions,[13f] in which the *strain* (i.e., the energy needed to promote the reactants from their equilibrium geometries to the geometries they adopt in the transition sates), controls the process despite the highly aromatic character of the corresponding saddle points. The so-called strain is also the major contributor in controlling the activation barriers of other pericyclic reactions like [3+2] or [4+2] cycloadditions,[17,18] so we can speculate that this factor plays also an important role in controlling the barrier energies of the [4+3] cycloaddition reactions considered in this report.

Cycloadditions with furan as diene: Finally, we were interested in the effect of the metal fragment when the cycloaddition of the tethered allenes occur with furan as diene instead of 1,3-butadiene. Therefore, we first computed the cycloaddition reaction of the parent oxyallylic cation, **3j**. Contrary to cation **3a**, the transformation **3j→4j** is not concerted but proceeds stepwise through the formation of the σ complex **5j** (Scheme 3).

Similar to **3j**, the Pt^{II} complex **3k** also evolves to the final carbenoid complex **4k** through a stepwise reaction mechanism via the formation of the corresponding σ complex **5k**. As readily seen in Scheme 4, both steps of the transformation are more difficult for complex **3k** than for cation **3j**, if we take into account the computed barrier energies. Moreover, the second reaction step of the metal-assisted process

Table 2. Calculated $\Delta G^{\neq}_{298}$ [kcal mol^{-1}] for the cycloaddition reaction of **3a**,**d**,**i** in different solvents. All values were calculated at the B3LYP/def2-SVP level.

ε (solvent)	$\Delta G^{\neq}_{298}$ (complex **3a**)	$\Delta G^{\neq}_{298}$ (complex **3d**)	$\Delta G^{\neq}_{298}$ (complex **3i**)
1.00 (gas phase)	0.7	10.7	4.8
7.43 (THF)	0.9	11.8	4.1
35.67 (acetone)	1.0	12.0	4.0

Scheme 3. Stepwise [4+3] cycloaddition of cation **3j**. Bond lengths are given in Å and energies (placed close to arrows) in kcal mol^{-1}. See Scheme 2 legend for additional details.
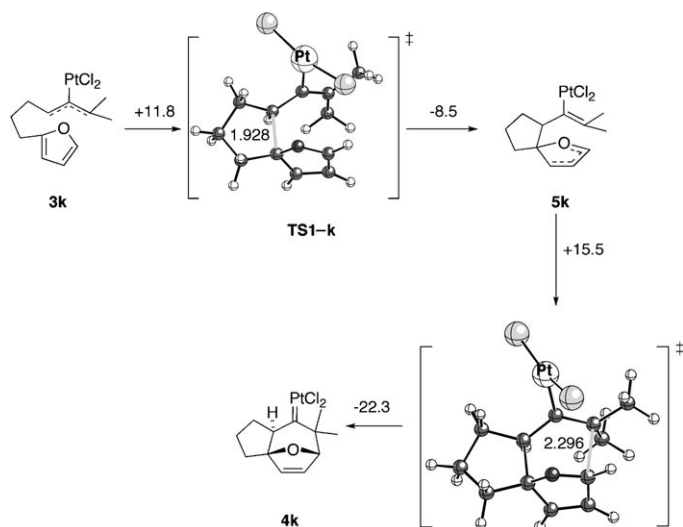
Scheme 4. Stepwise [4+3] cycloaddition of Pt^{II} complex **3k**. Bond lengths are given in Å and energies (placed close to arrows) in kcal mol^{-1}. See Scheme 2 legend for additional details.

is exothermic, which is different to that for the non-organometallic cation **3j**. Despite these differences, it is clear that the presence of the metal moiety does not alter the topology of the reaction coordinate, which is mainly dominated by the diene in the considered cycloaddition reactions.

This is in agreement with previous calculations reported by Harmata and Schreiner[19] and by Cramer and co-workers[10] who concluded that reactive and strongly electrophilic allylic cations and nucleophilic dienes tend to react through stepwise mechanisms, while less electrophilic cations and less nucleophilic dienes tend to react through concerted processes. We examined this hypothesis by computing the electrophilicities ω^+ of allylic species **6a** and **6b**, as well as the
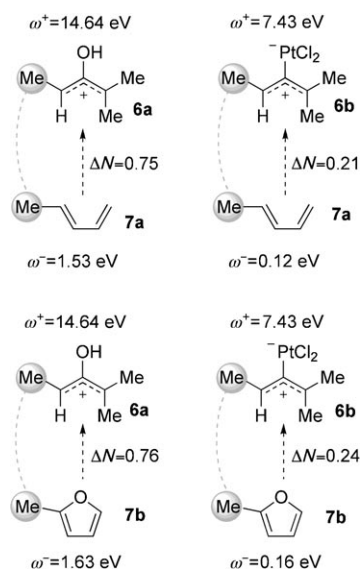
Scheme 5. Electrophilicities (ω^+), nucleophilicities (ω^-) and charge transfers (ΔN) computed for the intermolecular interaction between allylic systems **6a,b** and dienes **7a,b**. Dotted lines indicate the connection between these interactions and those present in **3a** (**6a+7a**), **3i** (**6b+7a**), **3j** (**6a+7b**) and **3k** (**6b+7b**).

nucleophilicities ω^- of dienes **7a** and **7b** (Scheme 5). These intermolecular systems incorporate the main geometric and electronic features of reactants **3a**, **3i**, **3j**, and **3k** (Scheme 4).

The electrophilicities were computed by using the following formula:[20]

$$\omega^+ = \frac{\mu^2}{2\eta} \tag{2}$$

where μ and η are the chemical potential and hardness of species **6a,b**, respectively. Similarly, the nucleophilicity indexes of species **7a,b** (denoted as A) with respect to electrophiles **6a,b** (denoted as B) were calculated by using the following conceptually related expression:[21]

$$\omega^-_{A\to B} = \frac{1}{2} \frac{(\mu_A - \mu_B)^2}{(\eta_A + \eta_B)^2} \eta_A \tag{3}$$

The charge transfers $\Delta N_{A\to B}$ from nucleophiles A to electrophiles B were estimated by the following equation:[22]

$$\Delta N_{A\to B} = \frac{\mu_A - \mu_B}{\mu_A + \mu_B} \tag{4}$$

The chemical potentials and hardness of the involved species were calculated within the following approximations:[20a,23]

$$\mu = -\frac{I+A}{2} \approx \frac{\varepsilon_{HOMO} - \varepsilon_{LUMO}}{2} \tag{5}$$

$$\eta = I - A \approx \varepsilon_{LUMO} - \varepsilon_{HOMO} \qquad (6)$$

In these latter equations, I and A stand for the ionization potential and electron affinity, respectively, and ε_{HOMO} and ε_{LUMO} are the orbital energies of the corresponding frontier orbitals.

As seen in Scheme 5, cationic species **6a** is much more electrophilic than neutral reactant **6b**. In addition, 2-methylfuran **7b** is more nucleophilic toward both **6a** and **6b** than 1,3-pentadiene **7a**. Accordingly, the ΔN values are slightly higher in the case of **7b**. Therefore, we can conclude that in the case of the more nucleophilic furane dienes there is a higher charge transfer with respect to both electrophiles **6a,b**, a result which parallels the stepwise character of [3+4] reactions involving the furan moiety, although the differences on going from **7a** to **7b** are quite low.

In order to gain a deeper understanding of the reasons for this transit from concerted to stepwise cycloadditions, we analyzed in more detail the behavior of the parent reactions involving hydroxy reactants **3a** and **3j**. If the stepwise mechanism is considered, the first step consists of a nucleophilic attack of C7 to C3, with an electronic displacement to generate an enol moiety (Figure 5). In the case of a concerted $[_\pi 4_s + _\pi 2_s]$ cycloaddition, interaction between both C3–C7 and C1–C10 pairs is required, through the corresponding MOs in which appropriate symmetries ensure a cyclic electronic delocalization associated with an aromatic transition structure (Figure 5).
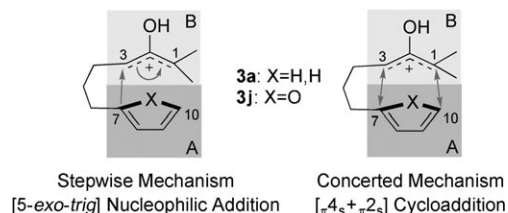

Figure 5. Main two-electron interactions involved in concerted and stepwise [4+3] cycloadditions of reactants **3a** and **3j**.

The potential energy surfaces corresponding to the respective reactions, as well as the stationary points and one early point along the respective intrinsic reaction coordinates, are shown in Figure 6.

A relaxed scan of the possible reaction paths (Figure 6 A) for **3a** reveals a smooth surface in which only **TSa** can be found as a saddle point connecting **3a** and the [4+3] product **4a** through an *intramolecular* concerted mechanism. This result contrasts with those found by Cramer and Barrows, who found a stepwise mechanism in the *intermolecular* [4+3] reaction between 2-hydroxyallyl cation and 1,3-butadiene.[10b] A similar inspection of the projected potential energy surface for the **3j**→**4j** transformation (Figure 6 B) reveals a stepwise mechanism with intermediate **5j** connecting reactant and product via **TS1j** and **TS2j**.
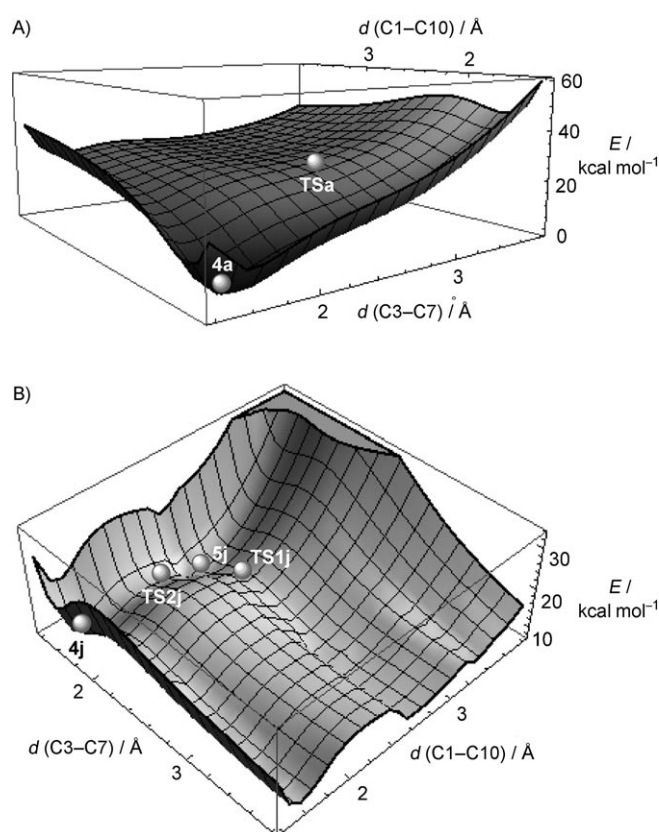

Figure 6. Potential energy hypersurfaces (B3LYP/def2-SVP//B3LYP/6-31G* level) projected on the C1–C2 and C3–C4 bond lengths associated with the [4+3] cycloaddition reactions of: A) **3a**, and B) **3j**. The stationary points corresponding to transition structures and intermediates are shown as spheres.

In order to analyze the origins of these different profiles, we first studied the molecular orbitals of reactants **3a** and **3j**. These MOs are shown in Figure 7 and Figure 8, respectively. Since the chemical meaning of expansion coefficients in split-valence basis sets is difficult to determine, the respective orbital energies and expansion coefficients were recalculated by using the AM1 semiempirical Hamiltonian, so that the values could be used consistently (see below). From the main features of these figures, we can distinguish between MOs ϕ_1, ϕ_2, and ϕ_3 associated with the diene moieties and φ_1, φ_2, and φ_3, which are mainly delocalized within the allyl moieties of **3a** and **3j**. We can also observe that the main two-electron interactions, which are in principle compatible with a concerted symmetry-allowed [4+3] cycloaddition, are $\phi_2 \rightarrow \varphi_2$, $\phi_1 \rightarrow \varphi_3$, and $\phi_3 \rightarrow \varphi_1$. Given the electrophilic character of the allyl moieties, the latter interaction will be lower than the other two, corresponding to the HOMO–LUMO and HOMO−1–LUMO+1 two-electron interactions.

According to the second-order perturbation theory,[24] the contribution to the increase in energy on going to the reactant to the concerted TS associated with the intramolecular [4+3] cycloaddition can be decomposed into two terms. One is associated with the four-electron repulsion $E_{CON}^{(4)}$ be-
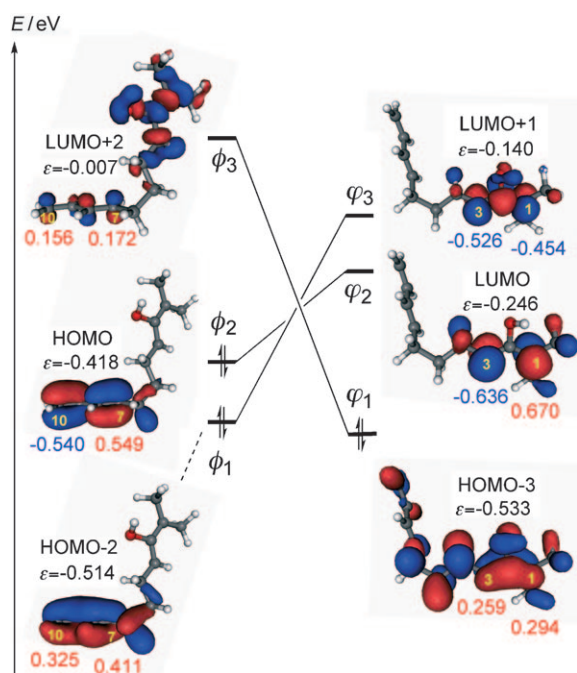
Figure 7. Significant molecular orbitals of reactant **3a**, computed at the RHF/AM1 level of theory.
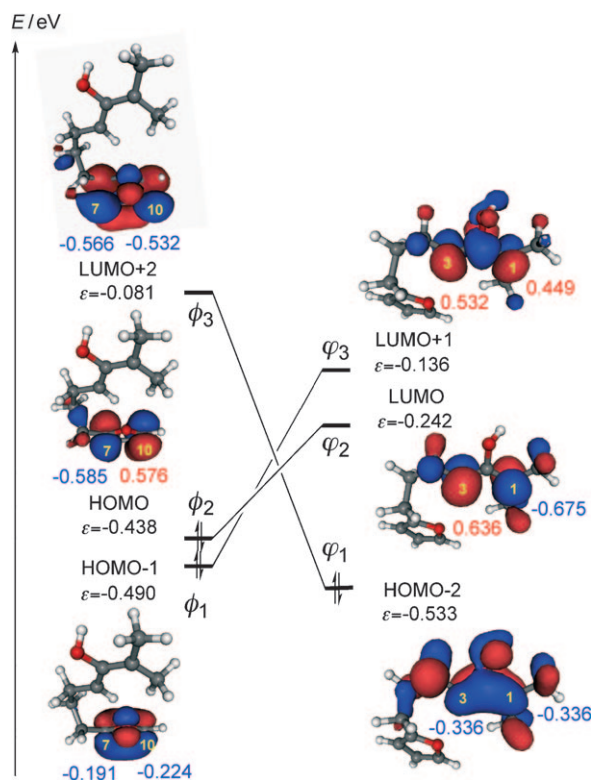

Figure 8. Significant molecular orbitals of reactant **3j**, computed at the RHF/AM1 level of theory.

tween the interacting carbon atoms, and the other is associated with the stabilizing two-electron interactions between these centers, which can in turn be decomposed as the con-

tributions of electron transfer from the diene A (Figure 5) to the allyl cation B, denoted as $E_{A \to B}^{(2)}$, and the reverse electron transfer from B to A $E_{B \to A}^{(2)}$, in order to complete the cyclic electronic circulation:

$$E_{CON} = E_{CON}^{(4)} + E_{A \to B}^{(2)} + E_{B \to A}^{(2)} \tag{7}$$

The four-electron term can be calculated as:

$$E_{CON}^{(4)} = -2(\beta_{1,10} S_{1,10} + \beta_{3,7} S_{3,7}) \tag{8}$$

where $\beta_{i,j}$ and $S_{i,j}$ are the resonance and overlap integrals between i and j carbon atoms, respectively. These integrals are connected by the Mulliken approach:

$$\beta_{i,j} = \frac{\beta_j^0 + \beta_j^0}{2} S_{i,j} \tag{9}$$

In Equation (9)—since we are considering only carbon atoms—$\beta_i^0 = \beta_j^0 = -178.01$ kcal mol^{-1}, which is the term optimized in the AM1 semiempirical Hamiltonian for a 2p carbon atom.[25]

The overlap integrals $S_{i,j}$ in Equations (8) and (9) can be calculated by using the Mulliken formula[26] for two interacting p-AOs:

$$S_{i,j} = \left[-1 - \zeta R_{i,j} - \frac{\zeta^2 R_{i,j}^2}{5} + 2\frac{\zeta^3 R_{i,j}^3}{15} + \frac{\zeta^4 R_{i,j}^4}{15} \right] \exp(-\zeta R_{i,j}) \tag{10}$$

In Equation (10) $R_{i,j}$ is the distance between atoms i and j and, according to the AM1 code,[25] $\xi = 3.185$ Å^{-1}.

According to second-order perturbation theory, the two-electron term corresponding to the A→B donation is given by the following expression:

$$E_{A \to B}^{(2)} = E_{\phi_2 \to \varphi_2}^{(2)} + E_{\phi_1 \to \varphi_3}^{(2)} = -2\frac{(c_7^{\phi_2} c_3^{\varphi_2} \beta_{7,3} + c_{10}^{\phi_2} c_1^{\varphi_2} \beta_{10,1})^2}{\varepsilon_{\varphi_2} - \varepsilon_{\phi_2}}$$
$$-2\frac{(c_7^{\phi_1} c_3^{\varphi_3} \beta_{7,3} + c_{10}^{\phi_1} c_1^{\varphi_3} \beta_{10,1})^2}{\varepsilon_{\varphi_1} - \varepsilon_{\phi_3}} \tag{11}$$

Similarly, the two-electron term corresponding to the B→A donation is given by the following expression:

$$E_{B \to A}^{(2)} = E_{\varphi_1 \to \phi_3}^{(2)} = -2\frac{(c_7^{\phi_3} c_3^{\varphi_1} \beta_{7,3} + c_{10}^{\phi_3} c_1^{\varphi_1} \beta_{10,1})^2}{\varepsilon_{\phi_3} - \varepsilon_{\varphi_1}} \tag{12}$$

In Equation (11) and (12), ϕ_n and φ_m MOs, with ε_{ϕ_n} and ε_{φ_m} orbital energies as well as $c_i^{\phi_n}$ and $c_j^{\varphi_m}$ expansion coefficients at atoms i and j, are denoted according to Figure 6 and Figure 7.

If the stepwise mechanism outlined in Figure 5 is considered, the first step associated with the nucleophilic attack of the diene subunit to the allyl moiety is given by:

$$E_{STP} = E_{STP}^{(4)} + E_{Nu}^{(2)} + E_{AB}^{Coul} \qquad (13)$$

Because during this stage only atoms C7 (of the nucleophile) and C3 (of the electrophile) are involved, the repulsive term of the first term on the right-hand side of Equation (13) reduces to:

$$E_{STP}^{(4)} = -2\beta_{7,3}S_{7,3} \qquad (14)$$

The two-electron stabilizing term associated with the nucleophilic attack is therefore:

$$E_{Nu}^{(2)} = -2\frac{\left(c_7^{\phi_2}c_3^{\varphi_2}\beta_{7,3}\right)^2}{\varepsilon_{\varphi_2} - \varepsilon_{\phi_2}} \qquad (15)$$

Finally, the electrostatic term corresponding to this nucleophilic addition is, in atomic units:

$$E_{AB}^{Coul} = \sum_{\substack{i \in A \\ j \in B}} \frac{q_i q_j}{R_{i,j}} \qquad (16)$$

where q_i and q_j are the charges of the respective atoms.[27]

We have evaluated the values of E_{CON} and E_{STP} for the values of $R_{i,j}$ corresponding to the early stages of the concerted and stepwise processes of **3a** and **3j**. We used Equations (7)–(16) and the values of the expansion coefficients and orbital energies gathered in Figures 7 and 8. The point charges (including the attached hydrogen atoms when necessary) were determined from the natural bonding analysis of each structure. The results thus obtained are shown in Figure 9.

According to our results, the stepwise mechanism is the preferred one along most of the potential energy surfaces associated with the initial stages of both **3a**→**4a** and **3j**→**4j** processes. This is due to the highly electrophilic character of the cationic allyl moiety of both reactants (Scheme 5), which results in low contributions of the $E_{B\rightarrow A}^{(2)}$ terms, thus hampering the cyclic electronic circulation required to complete the pericyclic mechanism. The most important two-electron stabilizing contribution stems from $E_{Nu}^{(2)}$, which is also the most important contribution to $E_{A\rightarrow B}^{(2)}$ in the concerted process. In the case of **3k**, the Coulombic term also contributes to a permanent preference for the stepwise mechanism, with the exception of one region associated with high values of the distance between C3 and C7 and low values for the C1−C10 distance (Figure 9B)—a geometry pattern that is not accessible to the intramolecular processes studied in this work. It is important to note that in the neighborhood of **TSa**, the concerted mechanism turns out to be the preferred one (Figure 9A), in nice agreement with our computational results for intramolecular [4+3] cycloadditions in which the distance between C3 and C7 is shorter than that between C1 and C10. In the case of intermolecular processes taking place through less restricted conformational spaces, the reaction would be stepwise, as it was found by Cramer and Barrows in their study on the intermolecular [4+3] cycload-
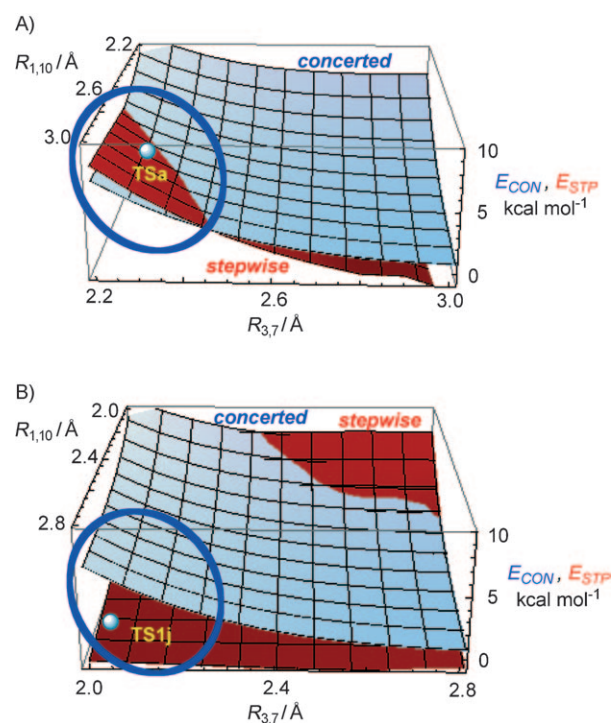

Figure 9. Plots of the interaction energies associated with the initial stages of the concerted (E_{CON}) and stepwise reactions (E_{STP}) of: A) **3a**, and B) **3j**. The energy values have been computed according to Equations (7)–(16); see main text for details. The terms $R_{1,10}$ and $R_{3,7}$ correspond to distances between the carbon atoms shown in Figure 5. In both diagrams, the neighborhood of the *intramolecular* transition structures is highlighted within a blue ellipse.

dition between 2-hydroxyallyl cation and 1,3-butadiene.[10b] Our model also suggests that in reactants possessing less electrophilic allyl moieties the region of the preferred concerted mechanism would be more extended.

Conclusion

From the computational study reported here the following conclusions can be drawn. 1) The studied thermal metal-mediated [4+3] cycloaddition reactions are concerted and take place via transition structures that can be even more synchronous and more aromatic than their non-organometallic analogues. 2) Despite that, the processes exhibit slightly to moderate higher activation barriers than the parent cycloaddition involving the hydroxyallyl cation. 3) The metal moiety induces a bond polarization in the initial reactants, which is related to the interaction of the transition metal with the allylic π* molecular orbital (LUMO). 4) Finally, the replacement of the 1,3-butadiene by furan causes the transformation to occur stepwise in both the non-organometallic and metal-assisted processes, the latter being more difficult based on the computed activation barriers. 5) In [4+3] reactions involving highly electrophilic allyl moieties there is a general preference for stepwise mechanisms with the exception of the region associated with *intramolecular* processes.

Computational Details

All the calculations reported here were obtained with the GAUSSIAN 03 suite of programs.[28] Electron correlation was partially taken into account by using the hybrid functional usually denoted as B3LYP[29] with the double-ζ quality plus polarization def2-SVP basis set[30] for all atoms. Zero point vibrational energy (ZPVE) corrections were computed at the B3LYP/def2-SVP level and were not scaled. Reactants and cycloadducts were characterized by frequency calculations,[23] and have positive definite Hessian matrices. Transition structures (TSs) show only one negative Eigenvalue in their diagonalized force constant matrices, and their associated Eigenvectors were confirmed to correspond to the motion along the reaction coordinate under consideration by using the intrinsic reaction coordinate (IRC) method.[31] Nonspecific solvent effects were described by using the self-consistent reaction field (SCRF) approach in its Onsager–Kirkwood formalism.[32] Nucleus independent chemical shifts (NICS)[7] were evaluated by using the gauge invariant atomic orbital[33] (GIAO) approach, at the GIAO-B3LYP/def2-SVP//B3LYP/def2-SVP level.

The synchronicity[34,35] of the reactions was quantified by using a previously described approach.[36] For a given concerted reaction, "synchronicity" is defined as:[37]

$$S_y = 1 - \frac{\sum\limits_{i=1}^{n} \frac{|\delta B_i - \delta B_{AV}|}{\delta B_{AV}}}{2n - 2} \quad (17)$$

where n is the number of bonds directly involved in the reaction (in this case, $n = 7$) and δB_i stands for the relative variation of a given bond index B_i at the transition state (TS), according to the following formula:

$$\delta B_i = \frac{B_i^{TS} - B_i^{R}}{B_i^{P} - B_i^{R}} \quad (18)$$

where the superscripts R and P refer to the reactants and the product, respectively. The average value of δB_i, denoted as δB_{AV}, is therefore:

$$\delta B_{AV} = n^{-1} \sum_{i=1}^{n} \delta B_i \quad (19)$$

The Wiberg bond indices[38] B_i and donor–acceptor interactions were computed by using the natural bond orbital (NBO)[39] method. The energies associated with these two-electron interactions were computed according to the following equation:

$$\Delta E_{\phi\phi*}^{(2)} = -n_\phi \frac{\left\langle \phi^* | \hat{F} | \phi \right\rangle^2}{\varepsilon_{\phi*} - \varepsilon_\Phi} \quad (20)$$

where $\hat{F}$ is the DFT equivalent of the Fock operator, and ϕ and ϕ^* are two filled and unfilled natural bond orbitals with ε_ϕ, y, $\varepsilon_{\phi*}$ energies, respectively; n_ϕ stands for the occupation number of the filled orbital.

Acknowledgements

[1] For reviews on [4+3] cycloaddition chemistry, see: a) J. H. Rigby, F. C. Pigge, *Org. React.* **1997**, *51*, 351; b) M. Harmata, *Adv. Cycloaddit.* **1997**, *4*, 41; c) M. Harmata, *Recent Res. Dev. Org. Chem.* **1997**, *1*, 523; d) M. Harmata, *Tetrahedron* **1997**, *53*, 6235; e) J. K. Cha, J. Oh,

[2] Some recent examples: a) G. Prié, N. Prévost, H. Twin, S. A. Fernandes, J. F. Hayes, M. Shipman, *Angew. Chem.* **2004**, *116*, 6679; *Angew. Chem. Int. Ed.* **2004**, *43*, 6517; b) J. Huang, R. P. Hsung, *J. Am. Chem. Soc.* **2005**, *127*, 50; c) J. E. Antoline, R. P. Hsung, J. Huang, Z. Song, G. Li, *Org. Lett.* **2007**, *9*, 1275, and references therein.

[3] Catalytic examples of direct [4C+3C] cycloadditions are very rare and essentially limited to the use of furan as the 4C partner; see: a) M. Harmata, S. K. Ghosh, X. Hong, S. Wacharasindhu, P. Kirchhoefer, *J. Am. Chem. Soc.* **2003**, *125*, 2058; b) M. Harmata, J. A. Brackley III, C. L. Barnes, *Tetrahedron Lett.* **2006**, *47*, 8151; c) see also reference [2].

[4] B. Trillo, F. López, M. Gulías, L. Castedo, J. L. Mascareñas, *Angew. Chem.* **2008**, *120*, 965; *Angew. Chem. Int. Ed.* **2008**, *47*, 951.

[5] a) B. Trillo, F. López, S. Montserrat, G. Ujaque, L. Castedo, A. Lledós, J. L. Mascareñas, *Chem. Eur. J.* **2009**, *15*, 3336; b) I. Alonso, B. Trillo, F. López, S. Montserrat, G. Ujaque, L. Castedo, A. Lledós, J. L. Mascareñas, *J. Am. Chem. Soc.* **2009**, *131*, 13020; c) D. Benitez, E. Tkatchouk, A. Z. Gonzalez, W. A. Goddard, F. D. Toste, *Org. Lett.* **2009**, *11*, 4798; d) P. Mauleon, R. M. Zeldin, A. Z. González, F. D. Toste, *J. Am. Chem. Soc.* **2009**, *131*, 6348.

[6] a) H. Jiao, P. von R. Schleyer, *J. Phys. Org. Chem.* **1998**, *11*, 655; b) P. von R. Schleyer, H. Jiao, *Pure Appl. Chem.* **1996**, *68*, 209, and references therein.

[7] Z. Chen, C. S. Wannere, C. Corminboeuf, R. Puchta, P. von R. Schleyer, *Chem. Rev.* **2005**, *105*, 3842.

[8] I. Fernández, M. A. Sierra, F. P. Cossío, *J. Org. Chem.* **2006**, *71*, 6178.

[9] a) I. Fernández, M. A. Sierra, F. P. Cossío, *J. Org. Chem.* **2008**, *73*, 2083; b) see also the featured article: M. A. Sierra, I. Fernández, F. P. Cossío, *Chem. Commun.* **2008**, 4671.

[10] a) C. J. Cramer, S. E. Barrows, *J. Phys. Org. Chem.* **2000**, *13*, 176; b) C. J. Cramer, S. E. Barrows, *J. Org. Chem.* **1998**, *63*, 5523.

[11] We also tried to compute the [4+3] cycloaddition reaction in the corresponding neutral oxyallyl species in a similar way to **3a**. However, we found that this compound only exists as a biradical species and is the corresponding cyclopropanone that is ca. 14 kcal mol⁻¹ lower in energy. A similar result has been quite recently found by Houk, Hsung and co-workers in a similar system: E. H. Krenske, K. N. Houk, A. G. Lohse, J. E. Antoline, R. P. Hsung, *Chem. Sci.* **2010**, *1*, 387. This biradical species **3a′** can also undergo the cycloaddition process with an activation barrier of 5.6 kcal mol⁻¹.

[12] R. F. W. Bader, *Atoms in Molecules-A Quantum Theory*, Clarendon Press, Oxford, **1990**, pp. 12–52.

[13] a) I. Morao, B. Lecea, F. P. Cossío, *J. Org. Chem.* **1997**, *62*, 7033; b) F. P. Cossío, I. Morao, H. Jiao, P. von R. Schleyer, *J. Am. Chem. Soc.* **1999**, *121*, 6737; c) I. Fernández, M. A. Sierra, F. P. Cossío, *J. Org. Chem.* **2007**, *72*, 1488; d) I. Fernández, F. P. Cossío, M. A. Sierra, *Organometallics* **2007**, *26*, 3010; e) G. Frenking, F. P. Cossío, M. A. Sierra, I. Fernández, *Eur. J. Org. Chem.* **2007**, 5410; f) I. Fernández, F. P. Cossío, F. M. Bickelhaupt, *Chem. Eur. J.* **2009**, *15*, 13022.

[14] H. Fallah-Bagher-Shaidaei, C. S. Wannere, C. Corminboeuf, R. Puchta, P. von R. Schleyer, *Org. Lett.* **2006**, *8*, 863.

[15] a) R. Herges, D. Geuenich, *J. Phys. Chem. A* **2001**, *105*, 3214; b) D. Geuenich, K. Hess, F. Köhler, R. Herges, *Chem. Rev.* **2005**, *105*, 3758.

[16] a) P. von R. Schleyer, H. Jiao, M. N. Glukhoutsev, J. Chandrasekhar, E. Kraka, *J. Am. Chem. Soc.* **1994**, *116*, 10129; b) P. von R. Schleyer, H. Jiao, *Pure Appl. Chem.* **1996**, *68*, 209, and references therein.

[17] D. H. Ess, K. N. Houk, *J. Am. Chem. Soc.* **2008**, *130*, 10187.

[18] A. E. Hayden, K. N. Houk, *J. Am. Chem. Soc.* **2009**, *131*, 4084.

[19] M. Harmata, P. R. Schreiner, *Org. Lett.* **2001**, *3*, 3663.

[20] a) R. G. Parr, L. Szentpály, S. Liu, *J. Am. Chem. Soc.* **1999**, *121*, 1922; b) A. T. Maynard, M. Huang, W. G. Rice, D. G. Covell, *Proc. Natl. Acad. Sci. USA* **1998**, *95*, 11578.

[21] P. Jaramillo, P. Pérez, R. Contreras, W. Tiznado, P. Fuentealba, *J. Phys. Chem. A* **2006**, *110*, 8181.

[22] a) R. G. Parr, W. Yang, *Density Functional Theory of Atoms and Molecules*, Oxford Science Publications, Oxford, **1989**; b) J. G. Malone, *J. Chem. Phys.* **1933**, *1*, 197.

[23] J. W. McIver, Jr., A. Komornicki, *J. Am. Chem. Soc.* **1972**, *94*, 2625.

[24] a) L. Salem, *J. Am. Chem. Soc.* **1968**, *90*, 543; b) L. Salem, *J. Am. Chem. Soc.* **1968**, *90*, 223.

[25] M. J. S. Dewar, E. G. Zoebisch, E. F. Healy, J. J. P. Stewart, *J. Am. Chem. Soc.* **1985**, *107*, 3902.

[26] R. S. Mulliken, C. A. Rieke, D. Orloff, H. Orloff, *J. Chem. Phys.* **1949**, *17*, 1248.

[27] S. Vivanco, B. Lecea, A. Arrieta, P. Prieto, I. Morao, A. Linden, F. P. Cossío, *J. Am. Chem. Soc.* **2000**, *122*, 6078.

[28] Gaussian 03, Revision D.01, M. J. Frisch, G. W. Trucks, H. B. Schlegel, G. E. Scuseria, M. A. Robb, J. R. Cheeseman, J. A. Montgomery, Jr., T. Vreven, K. N. Kudin, J. C. Burant, J. M. Millam, S. S. Iyengar, J. Tomasi, V. Barone, B. Mennucci, M. Cossi, G. Scalmani, N. Rega, G. A. Petersson, H. Nakatsuji, M. Hada, M. Ehara, K. Toyota, R. Fukuda, J. Hasegawa, M. Ishida, T. Nakajima, Y. Honda, O. Kitao, H. Nakai, M. Klene, X. Li, J. E. Knox, H. P. Hratchian, J. B. Cross, V. Bakken, C. Adamo, J. Jaramillo, R. Gomperts, R. E. Stratmann, O. Yazyev, A. J. Austin, R. Cammi, C. Pomelli, J. W. Ochterski, P. Y. Ayala, K. Morokuma, G. A. Voth, P. Salvador, J. J. Dannenberg, V. G. Zakrzewski, S. Dapprich, A. D. Daniels, M. C. Strain, O. Farkas, D. K. Malick, A. D. Rabuck, K. Raghavachari, J. B. Foresman, J. V. Ortiz, Q. Cui, A. G. Baboul, S. Clifford, J. Cioslowski, B. B. Stefanov, G. Liu, A. Liashenko, P. Piskorz, I. Komaromi, R. L. Martin, D. J. Fox, T. Keith, M. A. Al-Laham, C. Y. Peng, A. Nanayakkara, M. Challacombe, P. M. W. Gill, B. Johnson, W. Chen, M. W. Wong, C. Gonzalez, J. A. Pople, Gaussian, Inc., Wallingford CT, **2004**.

[29] a) A. D. Becke, *J. Chem. Phys.* **1993**, *98*, 5648; b) C. Lee, W. Yang, R. G. Parr, *Phys. Rev. B* **1988**, *37*, 785; c) S. H. Vosko, L. Wilk, M. Nusair, *Can. J. Phys.* **1980**, *58*, 1200.

[30] F. Weigend, R. Alhrichs, *Phys. Chem. Chem. Phys.* **2005**, *7*, 3297.

[31] C. González, H. B. Schlegel, *J. Phys. Chem.* **1990**, *94*, 5523.

[32] a) L. Onsager, *J. Am. Chem. Soc.* **1936**, *58*, 1486; b) M. W. Wong, K. B. Wiberg, M. J. Frisch, *J. Am. Chem. Soc.* **1992**, *114*, 523; c) M. W. Wong, K. B. Wiberg, M. J. Frisch, *J. Am. Chem. Soc.* **1992**, *114*, 1645.

[33] K. Wolinski, J. F. Hilton, P. Pulay, *J. Am. Chem. Soc.* **1990**, *112*, 8251.

[34] a) M. J. S. Dewar, *J. Am. Chem. Soc.* **1984**, *106*, 209; b) W. T. Borden, R. J. Loncharich, K. N. Houk, *Annu. Rev. Phys. Chem.* **1988**, *39*, 213.

[35] Leroy has proposed the term "asynchronism" in similar contexts. See: G. Leroy, M. Sana, *Tetrahedron* **1975**, *31*, 2091.

[36] A. Moyano, M. A. Pericás, E. Valentí, *J. Org. Chem.* **1989**, *54*, 573.

[37] a) B. Lecea, A. Arrieta, G. Roa, J. M. Ugalde, F. P. Cossío, *J. Am. Chem. Soc.* **1994**, *116*, 12314; b) B. Lecea, A. Arrieta, X. López, J. M. Ugalde, F. P. Cossío, *J. Am. Chem. Soc.* **1995**, *117*, 12314.

[38] K. B. Wiberg, *Tetrahedron* **1968**, *24*, 1083.

[39] a) J. P. Foster, F. Weinhold, *J. Am. Chem. Soc.* **1980**, *102*, 7211; b) A. E. Reed, F. Weinhold, *J. Chem. Phys.* **1985**, *83*, 1736; c) A. E. Reed, R. B. Weinstock, F. Weinhold, *J. Chem. Phys.* **1985**, *83*, 735; d) A. E. Reed, L. A. Curtiss, F. Weinhold, *Chem. Rev.* **1988**, *88*, 899.